Journal of Orthopaedic Research

SHOX GENE IS EXPRESSED IN VERTEBRAL BODY GROWTH PLATES IN IDIOPATHIC AND CONGENITAL SCOLIOSIS: IMPLICATIONS FOR THE AETIOLOGY OF SCOLIOSIS IN TURNER SYNDROME.

Journal:	*Journal of Orthopedic Research*
Manuscript ID:	draft
Wiley - Manuscript type:	Research Article
Date Submitted by the Author:	n/a
Complete List of Authors:	Day, Gregory; Griffith University, Genomics Research; Bond University, Orthopaedic Surgery Szvetko, Attila; Griffith University, Genomics Research Griffiths, Lyn; Griffith University, Research Institute McPhee, Ian; University of Queensland, Orthopaedics Tuffley, John; Royal Children's Hospital, Orthopaedics Labrom, Robert; Royal Children's Hospital, Orthopaedics Askin, Geoffrey; Mater Children's Hospital, Orthopaedics Woodland, Peter; Princess Margaret Hospital for Children, Orthopaedic Surgery McClosky, Eamonn; Princess Margaret Hospital for Children, Orthopaedic Surgery Ian, Torode; Royal Children's Hospital, Orthopaedic Surgery Tomlinson, Francis; University of Queensland, Surgery
Keywords:	SHOX, Gene, exprssion, scoliosis

SHOX GENE IS EXPRESSED IN VERTEBRAL BODY GROWTH PLATES IN IDIOPATHIC AND CONGENITAL SCOLIOSIS: IMPLICATIONS FOR THE AETIOLOGY OF SCOLIOSIS IN TURNER SYNDROME.

Gregory Day[1,2,7], Attila Szvetko[2], Lyn Griffiths[2], I Bruce McPhee[1], John Tuffley[3], Robert LaBrom[3], Geoffrey Askin[4], Peter Woodland[5], Eamonn McClosky[5], Ian Torode[6], Francis Tomlinson[1].

University of Queensland, Department of Surgery[1]

Griffith University, Genomics Research Centre[2]

Royal Children's Hospital, Queensland[3]

Mater Children's Hospital, Brisbane[4]

Princess Margaret Hospital for Children, Perth[5]

Royal Children's Hospital, Melbourne[6]

Bond University[7]

Abstract

Background

Reduced SHOX gene expression has been demonstrated to be associated with all skeletal abnormalities in Turner syndrome, other than scoliosis (and kyphosis). There is evidence to suggest that Turner syndrome scoliosis is clinically and radiologically similar to idiopathic scoliosis, although the phenotypes are dissimilar.

Study Design and Aims

This pilot gene expression study used relative quantitative real-time PCR (qRT-PCR) of the SHOX (Short Stature on X) gene to determine whether it is expressed in vertebral body growth plates in idiopathic and congenital scoliosis.

Methods

After vertebral growth plate dissection, tissue was examined histologically and RNA was extracted and its integrity was assessed using a Bio-Spec Mini™, NanoDrop® ND-1000 spectrophotometer and standard denaturing gel electrophoresis. Following cDNA synthesis, gene-specific optimization in a Corbett RotorGene 6000 real-time cycler was followed by qRT-PCR of vertebral tissue.

Results

Histological examination of vertebral samples confirmed that only growth plate was analysed for gene expression. Cycling and melt curves were resolved in triplicate for

all samples. SHOX abundance was demonstrated in congenital and idiopathic scoliosis vertebral body growth plates. SHOX expression was 11-fold greater in idiopathic compared to congenital (N=3) scoliosis (p=0.027).

Discussion and Significance

This study confirmed that SHOX was expressed in vertebral body growth plates, which implies that its expression may also be associated with the scoliosis (and kyphosis) of Turner syndrome. SHOX expression is reduced in Turner syndrome (short stature). In this study, increased SHOX expression was demonstrated in idiopathic scoliosis (tall stature) and congenital scoliosis.

Acknowledgements

This study was partly funded by a grant from the Australian Orthopaedic Association Research Foundation (#008RF) and an ARC Linkage grant in collaboration with Corbett Research (LP0455069).

Background

SHOX Gene, Turner Syndrome Phenotype and Scoliosis

The SHOX (short stature on X) homeobox gene was discovered in 1997.[1] Homeobox genes are known to regulate development. SHOX is located on the pseudo-autosomal region (PAR) of the short arms of the X and Y chromosomes. During meiosis, a high frequency of recombination of the short arms of both the X and Y chromosomes occurs, predisposing to terminal deletions, mutations and duplications.[2,3,4,5] Haploinsufficiency, (less than normal complement, eg. due to absence of one X chromosome) of the SHOX gene results in reduced expression and mesomelic short stature. Syndromes associated with SHOX gene abnormalities/deletions/mutations include idiopathic short stature, Leri-Weill, Langer and Turner syndrome (TS). Characteristic dysmorphic skeletal features of Turner, Leri-Weill and Langer syndromes include micrognathia (60%), cubitus valgus (47%), high-arched palate (38%), short fourth metacarpal (37%), webbed neck (25%) and Madelung deformity (7%).[6,7,8] Scoliosis typical of the idiopathic-type (up to 28%) and kyphosis (20%) are also evident in Turner syndrome.[9-12] SHOX gene haploinsufficiency has been linked to all the skeletal features of Turner syndrome except the scoliosis (and kyphosis). SHOX gene overdosage (greater than the normal complement), with increased

expression, is associated with tall stature in Turner Syndrome (gonadal dysgenesis).[13,14]

SHOX Gene Influence on Phenotype

The observed stature changes and dysmorphic skeletal features in Turner syndrome imply that the SHOX gene influences the timing of growth plate fusion and skeletal maturation.[15] SHOX gene is expressed in the middle aspect (mesomelic region) of the upper limbs and the pharyngeal arch and has undetectable expression in embryonic somites which eventually form vertebrae.[6] Because reduced expression of SHOX is associated with skeletal growth plate dysmorphism in Turner syndrome, there is reason to postulate that the same gene abnormality is associated with Turner syndrome scoliosis (and kyphosis). To date, no data regarding SHOX gene expression in vertebral growth plates in Turner syndrome or other conditions is known. The molecular mechanism of SHOX influence on bone development is unknown.[16]

Typical Phenotype of Idiopathic Scoliosis

Females with idiopathic scoliosis have tall stature.[17-23] The majority of females with thoracic scoliosis also have a thoracic hypokyphosis, indicating possible relative overgrowth of the thoracic vertebral bodies, compared to the posterior elements of the thoracic spine.[24-28] Over-stimulation of the vertebral growth plates before the onset of adolescence could explain these findings.[29] Delayed puberty with delayed skeletal maturation have been implicated as risk factors for the progression of idiopathic scoliosis.[30-32] It is now generally accepted that skeletal growth is a significant contributing factor to the development and natural history of idiopathic scoliosis.[33,34]

Comparison of Scoliosis of the Idiopathic Type and Turner Syndrome

The scoliosis in Turner syndrome is clinically and radiologically so similar to idiopathic scoliosis, that questions regarding a similar etiology have been raised.[9-12] Turner syndrome scoliosis is usually not severe enough to require surgery, limiting the opportunity to acquire cartilage from the vertebral body growth plates.[35-37] However, routine surgery for idiopathic and congenital scoliosis provides that opportunity for the acquisition of vertebral body growth plates for analysis of SHOX gene expression.

Study Aim and Design

Normative data of SHOX gene expression in the vertebral body growth plates of a control female adolescent population is lacking. This study aimed to determine whether SHOX is expressed in vertebral body growth plates and to compare SHOX expression in idiopathic scoliosis versus congenital scoliosis, which demonstrate dissimilar phenotypes.[38-40] Relative quantitative real-time PCR (qRT-PCR) characterized gene expression profiles for SHOX in tissue samples obtained surgically from vertebral body growth plate cartilage of idiopathic and congenital scoliotic patients as well as skeletal muscle from healthy controls (a tissue known to be abundant in SHOX).[41] qRT-PCR's specificity and sensitivity make this technology the current benchmark for high-quality, reproducible detection and comparison of gene expression.[42]

Materials and Methods

Patients and Tissues

Samples were collected from three females with idiopathic scoliosis and two males/one female with congenital scoliosis, as well as skeletal muscle as a positive SHOX control. Paravertebral skeletal muscle was collected from four healthy control patients. Patient demographics including diagnosis, age at the time of surgery and gender are listed in Table 1. Radiographs of the congenital and idiopathic scoliotic deformities from which the tissues were obtained are illustrated in Figures 1,2.

Tissue Harvesting

Fresh vertebral body growth plates from three patients with idiopathic scoliosis and three with congenital scoliosis were harvested at the time of scoliosis surgery. The vertebral body growth plate was sheared from the underlying vertebral body by sharp dissection (convex side) and curette (concave side of the curve), which revealed a thin layer of growth plate between the intervertebral disc and the end-plate of the vertebral body. Part of each specimen was immediately placed in Histochoice™ solution (Amresco) for a period of 72 hours to preserve cartilage whilst the other part (0.5-1.5g) was immediately frozen in sterile vials on dry ice for RNA extraction. The tissue in Histochoice™ solution was subsequently stored in 70% ethanol.

Fresh skeletal muscle was harvested from the paraspinal area of four healthy patients undergoing a variety of spine surgery procedures and sterile vials were also

immediately deposited on dry ice. Institutional Ethics permission was granted to store the specimens in a freezer at -80^0 C at the laboratory of the authors' Institution.

Tissue Dissection

All tissues were handled under surgically sterile conditions and dissected on fresh histology glass slides under a NIKON YS-100 dissecting microscope. Single-use disposable surgical blades were used for each tissue dissection. Care was taken during handling to avoid specimen contamination and thawing.

Histology

Histological examination of Haematoxylin & Eosin and Masson Trichrome stained paraffin-embedded sections 4-5µm thick demonstrated columns of chondrocytes adjacent to trabecular bone, characteristic of growth plate (Figures 3,4). An independent pathologist issued histology reports. Magnification images were recorded on analogue film and scanned, for clarity of reproduction (Figures 3,4). Histological examination of the skeletal muscle demonstrated macroscopically homogeneous muscle.

PCR Primer Design

The nucleotide sequences for SHOX were obtained using the gene search function at the National Centre for Biotechnology Information (NCBI) database. Isoform variants were assessed for functional relevance. Candidate regions for the transcripts of interest were assessed for priming, taking into account RNA thermodynamics using Mfold.[43] Primers were designed using the target specific alignment program Amplify (version 1.2).[44] *In Silico* prediction of primer dynamics was assessed using both that program and the UCSC *In Silico* PCR tool.[45] The non-redundant basic alignment tool, BLAST was used to ensure priming specificity.[46] Primers for SHOX were: 5' – GTT TGG TTC CAG AAC CGG AG – 3', reverse 5' – CTG TTG GAA AGG CAT CCG TA – 3'. Primers were obtained from GeneWorks Australia.

RNA Extraction

All equipment and work areas were initially treated with RNase Zap™ (Sigma). Tissues removed from the liquid nitrogen were immersed in 5-10mL Trizol™ homogenization reagent (Invitrogen) followed by short, high-speed homogenization

with a CAT tissue homogenizer (M Zipperer, Germany). Further tissue disintegration was performed using 23-gauge needles (Terumo). The homogenate was incubated for 5 minutes at 30°C to allow the complete dissociation of nucleoprotein complexes. Chloroform was then added (1.0-2.0mL) prior to vigorous agitation for 15 seconds, followed by another incubation period for 3 minutes at 30°C. Samples were transferred to 1.5mL tubes (Eppendorf) and centrifuged at 10,000rpm for 15 minutes at 4°C. Following centrifugation, the aqueous phase was transferred to a new sterile tube and RNA was precipitated with isopropanol (2.5-5mL). Samples were then incubated for 10 minutes at 30°C and subsequently centrifuged at 10,000rpm for 10 minutes at 4°C. The supernatant was then removed and the RNA pellet washed with 75% Ethanol (Analar) and then air-dried briefly. RNA purification was performed with an RNeasy™ Mini Kit (Qiagen). RNA was finally dissolved in UltraPure™ DNase/RNase-Free Distilled Water (Invitrogen).

RNA Integrity

RNA integrity was assessed using a Bio-Spec Mini™ spectrophotometer (Shimadzu), NanoDrop® ND-1000 spectrophotometer (NanoDrop Technologies) and standard denaturing gel electrophoresis. Spectrophotometric readings were obtained at neutral pH for absorbance at 260nm and 260:280nm with background correction of 320nm to allow for calculation of sample concentrations. Similarly, the ND-1000 spectrophotometer was used to calculate RNA concentration using 1uL of total sample. Results from the two spectrophotometers were compared. Standard formaldehyde agarose gel electrophoresis (FAG) was carried out with 1.2% gel to visualize the integrity of the total RNA obtained from extraction. Standard, molecular biology grade agarose (Promega), 10X FA gel buffer (3-N-morpholino-propanesulfonic acid, sodium acetate, ethylenediaminetetraacetic acid, sodium hydroxide, 37% (12.3M) formaldehyde), 1X FA running buffer (1X FA gel buffer, 2.5M formaldehyde), 5X RNA loading buffer (Bromophenol blue, ethylenediaminetetraacetic acid, formaldehyde, glycerol, formamide, 10X FA gel buffer), and UltraPure™ DNase/RNase-Free Distilled Water (Invitrogen) were used. RNA samples were incubated for 5 minutes at 70°C prior to loading for electrophoresis.

cDNA Synthesis

Each RNA sample was vortexed briefly to ensure homogenization and then heated to 55°C for 5 minutes. RNA was subjected to DNase treatment using DNaseI buffer, 0.1M DTT, and DNase I (2U/µL). DNase was heat inactivated at 65°C for 10 minutes. First strand synthesis of cDNA was achieved with SuperScript™ III (200U/µL) (Invitrogen). RNA (1-5µg) was converted using 5U/µL SuperScript™ III reverse transcriptase, reverse transcriptase buffer (50mM Tris-HCl pH 8.3, 75mM KCl, 3mM $MgCl_2$), 10mM dNTP mix, 10µM DTT, and 50ng/µL random hexamers. The mixture was first heated to 65°C for 5 minutes then incubated on ice for 1 minute. RNaseOUT™ (40U/µL) (Invitrogen) was added to each reaction. Thermal conditions for synthesis were 25°C for 10 minutes, then 50°C for 50 minutes, then 85°C for 5 minutes, followed by chilling on ice. RNase H (Invitrogen) was added to each cDNA sample. Three reactions were completed for quality assurance during cDNA synthesis. One reaction contained no reverse transcriptase, another contained no RNA, while the third contained genomic DNA. Products were resolved by standard agarose gel electrophoresis on 2% molecular biology grade agarose (Progen Biosciences) to verify purity and integrity. Generated cDNA samples were stored at -20°C.

qRT-PCR Optimization

Gene specific optimization on both human genomic DNA and human total RNA derived cDNA was performed. Optimal $MgCl_2$ concentrations and annealing temperatures were determined for the PCR primers. PCR primers were designed to be intron-spanning as an internal control facilitating the detection of genomic contaminants. An appropriate normalization gene was selected based on tissue specific expression profiles (18S). Conditions for the target genes and the reference gene were determined in unison to ensure uniformity. Cycling and melt curves were resolved using the Corbett Rotogene 6000 real-time cycler followed by standard gel electrophoresis to ensure only specific, expected products were produced during PCR.

Real-Time PCR

A Corbett Rotorgene 6000 platform performed relative quantitative real-time PCR. Each 25µL reaction contained 1X iQ™ SYBR® Green Supermix (Bio-Rad), 250nM forward and reverse primers, UltraPure™ DNase/RNase-Free Distilled Water (Invitrogen), 15nM Fluorosceine calibration dye, and 2µL patient cDNA. Cycling

conditions were: Cycle 1 (95°C for 3 minutes) X1, Cycle 2 (95°C for 30 seconds, 57°C for 30 seconds, 72°C for 30 seconds) X45, Cycle 3 (72°C for 4 minutes) X1, followed by melt curve resolution ramping 50°C to 99°C increasing 1°C every 5 seconds. Each reaction was executed in triplicate for the gene of interest, the reference gene and the no template control). A representative selection of amplified samples was resolved by standard agarose gel electrophoresis on 2% gels to check for specificity. Measuring gene specific PCR products provides an accurate means of determining mRNA relative abundance.[42] Cycling data was examined and a cycle-threshold (Ct) value was derived from the linear phase of each PCR from identical thresholds.

Statistical Analysis

Corbett Rotorgene 6000 software version 1.7 was used to generate and collate PCR data. Ct data was then exported to Microsoft Excel™ spreadsheets for further analysis. ΔΔCt methodology analyzed relative expression differences between idiopathic and congenital samples using 18S as the internal reference gene. Descriptive statistics were analyzed (including mean, SD, CV) taking into account triplicate reproducibility. Each patient sample's corresponding 18S Ct value was then subtracted and samples grouped. Grouped samples were then compared to each other to determine differences. Relative differences were calculated by applying the $2^{-\text{mean}(\Delta\Delta CT)}$ method according to previously published methods.[47] An independent samples T-test was then performed to determine the mean difference between congenital and idiopathic scoliosis at $\alpha=0.05$ (Table 2).

Results

RNA Integrity

Following RNA extraction, spectrophotometric yield and purity ratio were determined for total RNA for congenital and idiopathic scoliosis vertebral body growth plates (Table 3). Formaldehyde agarose gel electrophoretic patterns (FAG) were photographed to visually demonstrate total RNA from the vertebral body growth plate cartilage and the skeletal muscle. Results for the Bio-Spec Mini™ spectrophotometer

(Shimadzu) were comparable with the data from the NanoDrop® ND-1000 spectrophotometer (NanoDrop Technologies).

Real Time PCR Optimisation and cDNA Quality Assurance

Cycling and melt curves were resolved for muscle (Figure 5). Agarose gel electrophoretic patterns were photographed to visually demonstrate SHOX amplification in skeletal muscle (Figure 6). Cycling and melt curves were resolved for congenital and idiopathic scoliosis and analysed for the Ct values (Figures 7,8). Products of SHOX amplification from idiopathic and congenital scoliosis vertebral body growth plates were also resolved by standard agarose gel electrophoresis (Figure 9).

Gene Expression Analysis

Relative gene expression differences were calculated using 18S as a reference gene and by subtracting the Ct value of 18S from congenital and idiopathic scoliosis, before comparing them to each other. Although only three samples of vertebral growth plate for idiopathic and congenital scoliosis were analysed, there was minimal variation in real corrected Ct values for each type of analysed scoliosis sample (Table 4). Average Ct values for idiopathic and congenital scoliosis were calculated and compared. An 11-fold increase in SHOX expression was demonstrated in idiopathic compared to congenital scoliosis (Table 4). This result was statistically significant ($p=0.027$).

Comparison of Idiopathic and Congenital Scoliosis Groups

The mean age of patients in each group was calculated from age data in Table 1 at 12 years. The patients with idiopathic scoliosis were all female and two of the three patients with congenital scoliosis were male.

Discussion

SHOX Gene Location and Implications for Phenotypic Variability

SHOX gene is located on the pseudo-autosomal region (PAR) of the short arm of the X and Y chromosomes.[48] In females, one X chromosome is randomly selected for inactivation and appears as a Barr Body in the cell. The reason for this inactivation remains controversial. Genes on the PAR of the short arm of the X chromosome are

believed to escape X inactivation.[49] Active copies of SHOX are present on both X chromosomes and are required for normal phenotypic expression.[2] If terminal deletions/additions of the short arm of either the X or Y chromosome occur during meiosis (involving the locus for SHOX and adjacent genes), haploinsufficiency (reduced expression) or overdosage (increased expression) may result, and appear to be associated with a change in stature and dysmorphic skeletal features.

Significance of the Results

This was a novel gene expression study of the aetiology of scoliosis as it investigated a specific vertebral target tissue of a gene known to be associated with dysmorphic peripheral skeletal development in Turner syndrome. In this pilot study, SHOX was abundantly expressed in all scoliotic vertebral body growth plates. It is known that tissue-specific gene expression may be quantitatively altered by reactions to local changes, such as the development of scoliosis. Although the specimens were retrieved from scoliotic spines not associated with Turner syndrome, the fact that SHOX was expressed in vertebral body growth plates is a clue for future research regarding altered SHOX expression and the possible subsequent development of scoliosis. Future quantitated genetic expression studies may also assist in determining whether SHOX expression is altered by age or reaction to local changes. The exact mechanism of SHOX influence on growth plates is currently unknown.

References

1. Rao E, Weiss B, Fukami M, Rump A, Niesler B, Mertz A, Muroya K, Binder G, Kirsch S, Winkelmann M, Nordsiek G, Heinrich U, Breuning M, Ranke M, Rosenthal A, Ogata T, Rappold G. Pseudoautosomal deletions encompassing a novel homeobox gene cause growth failure in idiopathic short stature and Turner syndrome. Nat Genet. 1997;16:54-63.

2. Blaschke R, Rappold G. The pseudoautosomal regions, SHOX and disease. Curr Opin Genet Dev. 2006;16:233-239.

3. May C, Shone A, Kalaydjieva L, Sajantila A, Jeffreys A. Crossover clustering and rapid decay of linkage disequilibrium in the Xp/Yp pseudoautosomal gene SHOX. Nat Genet. 2002;31:272-275.

4. Filatov D, Gerrard D. High mutation rates in human and ape pseudoautosomal genes. Gene.2003;317:67-77

5. Graves J, Wakefield M, Toder R. The origin and evolution of the pseudoautosomal regions of human sex chromosomes. Hum Mol Genetics. 1998;7:1991-1996.

6. Clement-Jones M, Schiller S, Rao E, Blaschke RJ, Zuniga A, Zeller R, Robson SC, Binder G, Glass I, Strachan T, Lindsay S, Rappold GA. The short stature homeobox gene SHOX is involved in skeletal abnormalities in Turner syndrome. Hum Mol Genetics. 2000;9:695-702.

7. Ross J, Scott C Jn, Marttila P, Kowal K, Nass A, Papenhausen P, Abboudi J, Osterman L, Kushner H, Carter P, Ezaki M, Elder F, Wei F, Chen H, Zinn AR. Phenotypes associated with SHOX deficiency. J Clin Endocrin and Metab. 2001;86 (12): 5674-80.

8. Kosho T, Muroya K, Nagai T, Fujimoto M, Yokoya S, Sakamoto H, Hirano T, Terasaki H, Ohashi H, Nishimura G, Sato S, Matsuo N, Ogata T. Skeletal features and growth patterns in 14 patients with haploinsufficiency of SHOX: Implications for the development of Turner syndrome. J Clin Endocrin and Metab.1999;84 (12):4613-21.

9. Kim J., Rosenfeld S. and Keyak J. Increased Prevalence of Scoliosis in Turner syndrome. J Ped Orthopaedics. 2001;21:765-766.

10. Elder DA, Roper MG, Henderson RC, Davenport LM. Kyphosis in a Turner syndrome population. Pediatrics. 2002;109 (6); e93.

11. Day G, McPhee I B, Batch J, Tomlinson F**.** Growth rates and the prevalence and progression of scoliosis in short-statured children on Australian Growth Hormone programmes. Scoliosis J. 2007;2:3.

12. Day G, McPhee I B, Batch J. Scoliosis in growth hormone treated and non-treated Turner syndrome. Spine, e-Pub, 2004, Proceedings SSA.

13. Ogata T, Matsuo N, Nishimura G. SHOX Haploinsufficiency and overdosage: impact of gonadal function status. J Med Genet. 2001;38:1-6.

14. Ogata T, Inokuchi M, Ogawa M. Growth pattern and body proportion in a female with short stature homeobox containing gene overdosage and gonadal estrogen deficiency. Eur J Endocinol. 2002;147:249-254.

15. Kosho T, Muroya K, Nagai T, Fujimoto M, Yokoya S, Sakamoto H, Hirano T, Terasaki H, Ohashi H, Nishimura G, Sato S, Matsuo N, Ogata T. Skeletal features and growth patterns in 14 patients with haploinsufficiency of SHOX: Implications for the development of Turner syndrome. J Clin Endocrin and Metab. 1999;84:4613-21.

16. Marchini A, Rappold G, Schneider K. SHOX at a glance: from gene to protein.
Arch Physiol Biochem. 2007;113:116-123.

17. Willner S. A study of girls with adolescent idiopathic structural scoliosis. Clin Orthop Rel Res. 1974;101:129.

18. Buric M, Momcilovic B. Growth pattern and skeletal age in school-girls with idiopathic scoliosis. Clin Orthop Rel Res. 1982. 170:238-42.

19. Archer IA, Dickson RA. Stature and idiopathic scoliosis. A prospective study. J Bone Joint Surg. 1985. 67Br: 185-8.

20. Nicolopoulos KS, Burwell RG, Webb JK. Stature and its components in adolescent idiopathic scoliosis. J Bone Joint Surg. 1985. 67Br: 594-601.

21. Nordwall A, Willner S. A study of skeletal age and height in girls with Idiopathic scoliosis. Clin Orthop Rel Res. 1975. 110: 6-10.

22. Upadhyay SS, Hsu L, Ho E, Leong JCY, Lee M K. Disproportionate body growth in girls with adolescent idiopathic scoliosis. A longitudinal study. Spine. 1991;16(8 Suppl):S343-7.

23. Hagglund G, Karlberg J, Willner S. Growth in Girls with Adolescent Idiopathic Scoliosis. Spine 1992;17(1):108-111

24. Somerville E. Rotational lordosis: the development of the single curve. J Bone Joint Surg. 1952;34B:421-427.

25. Deane G., Duthie RB. A new projectional look at articulated scoliotic spines. Acta Orthop Scand. 1973. 44: 351-65.

26. Dickson R, Lawton J, Archer I, Butt W. The pathogenesis of idiopathic scoliosis. Biplanar spinal asymmetry. J Bone Joint Surg. 1984;66B:8-15.

27. Deacon P, Flood B, Dickson RA. Idiopathic scoliosis in three dimensions: a radiographic and morphometric analysis. J Bone Joint Surg.1984;66B:509-512.

28. Deacon P, Dickson R. Vertebral shape in the median sagittal plane in idiopathic thoracic scoliosis. A study of true lateral radiographs in 150 patients. Orthopedics. 1987;10:893-895.

29. Guo X, Chau W, Chan Y, Cheng J. Relative anterior spinal overgrowth in adolescent idiopathic scoliosis. Results of disproportionate endochondral membranous bone growth. J Bone Joint Surg. 2003;85B:1026-1031.

30. Lonstein J, Carlson J. The prediction of curve progression in untreated idiopathic scoliosis during growth. J Bone Joint Surg.1984;66A:1061-1071.

31. Drummond D, Rogala E. Growth and maturation of adolescents with idiopathic scoliosis. Spine. 1980;5:507-511.

32. Warren M, Brooks-Gunn J, Hamilton L, Warren L, Hamilton W. Scoliosis and fractures in young ballet dancers. Relation to delayed menarche and secondary amenorrhea. N Engl J Med. 1986;314:1348-1353.

33. Willner S. Adolescent idiopathic scoliosis : etiology. In Weinstein S (Ed) The Pediatric Spine: Principles and Practices. 1994:445-462. Raven Press, New York.

34. Goldberg C. Skeletal growth. Spine. State of the Art Reviews. 2000;14:401-409.

35. Ranke MB, Saenger P. Turner's syndrome. The Lancet. 2001. 358 (9278):309-14.

36. Batch J. Turner syndrome in childhood and adolescence. Best practice and Research. Clin Endocrin and Metab. 2002. 16 (3) :465-81.

37. Lippe B. Turner Syndrome. Endocrinology and Metabolism Clinics of North America. 1991; 20:121–152.

38. Giampietro P, Blank R, Raggio C, Merchant S, Jacobsen S, Faciszewski T, Shukla S, Greenlee A, Reynolds C, Schowalter D. Congenital and idiopathic scoliosis: Clinical and genetic aspects. Clin Med Res. 2003;1:125-136.

39. Maisenbacher M, Han J, O'Brien M, Tracy M, Erol B, Schaffer A, Dormans J, Zackai E, Kusumi K. Molecular analysis of congenital scoliosis: a candidate gene approach. Hum Genet. 205;116:416-419.

40. Giampietro P, Raggio C, Reynolds C, Shukla S, McPherson E, Ghebranious N, Jacobsen S, Kumar V, Faciszewski T, Pauli R, Rasmussen K, Burmester J, Zaleski C, Merchant S, David D, Weber J, Glurich I, Blank R. An analysis of PAX1 in the development of vertebral malformations. Clin Genet. 2005;68:448-453.

41. GeneCards. Website for the Weizmann Institute of Science. 2006.

42. Bustin SA, Benes V, Nolan T, Pfaffl MW. Quantitative real-time RT-PCR-a perspective. J Mol Endocrinol. 2005 343:597-601.

43. Zuker M. Mfold web server for nucleic acid folding and hybridisation prediction. Nucleic Acids Res. 2003 31:3406-3415.

44. Engels W. University of Wisconsin. Macintosh programme for simulating and testing PCRs. 1993-2005.

45. Kent J et al. The UCSC Genome Browser database: update 2006. Nucleic Acids Res. 2006; D590-D598.

46. Alscul S, Gish W, Miller W, Myers E, Lipman D. Basic local alignment search tool. J Mol Biol. 1990; 215:403-410.

47. Tajouri L, Mellick A, Tourtelotte A, Nagra R, Griffiths L. An examination of multiple sclerosis candidate genes identified as differentially regulated in multiple sclerosis plaque tissue, using absolute and comparative real-time Q-PCR analysis. Brain Res Protocols. 2005;15:79-91.

48. Rappold G. The pseudoautosomal regions of the human sex chromosomes. Hum Genet. 1993;92:315-324.

49. Carrel L, Willard H. X-inactivation profile reveals extensive variability in X-linked gene expression in females. Nature. 2005;434:400-404.

Table 1. Patient Demographics.

Patient	Gender	Age	Tissue	Clinical	Curve Type	Curve Angle
Idiopathic 1	F	13	Vertebral cartilage	Idiopathic scoliosis	Right thoracic	52
Idiopathic 2	F	13	Vertebral cartilage	Idiopathic scoliosis	Right thoracic	48
Idiopathic 3	F	10	Vertebral cartilage	Idiopathic scoliosis	Right thoracic	55
Congenital 1	M	16	Vertebral cartilage	Congenital scoliosis	Right thoracic	42
Congenital 2	F	12	Vertebral cartilage	Congenital scoliosis	Right Thoraco-lumbar	64
Congenital 3	M	9	Vertebral cartilage	Congenital scoliosis	Right thoracic	40
Tissue 1	M	32	Muscle	Spine fracture		
Tissue 2	F	17	Muscle	Spine fracture		
Tissue 3	M	53	Muscle	Spine infection		
Tissue 4	F	17	Muscle	Acute disc protrusion		

Figure 1. PA Plain Radiograph Congenital Scoliosis Patient # 3.

Figure 2. PA Plain Radiograph Idiopathic Scoliosis Patient # 3.

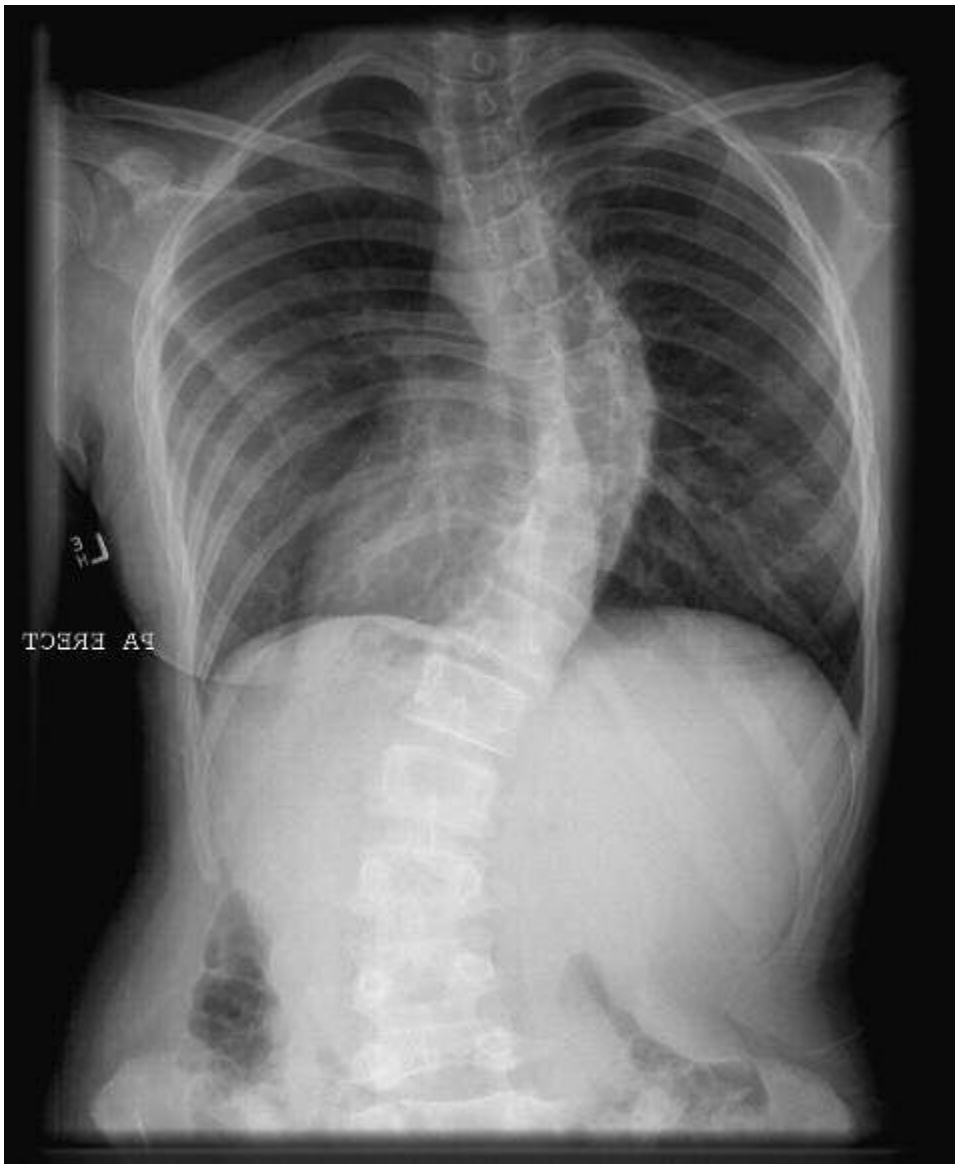

Figure 3. Haematoxylin & Eosin Stain x200 from Convex Side of Vertebral Body Growth Plate in Congenital Scoliosis Patient # 3.

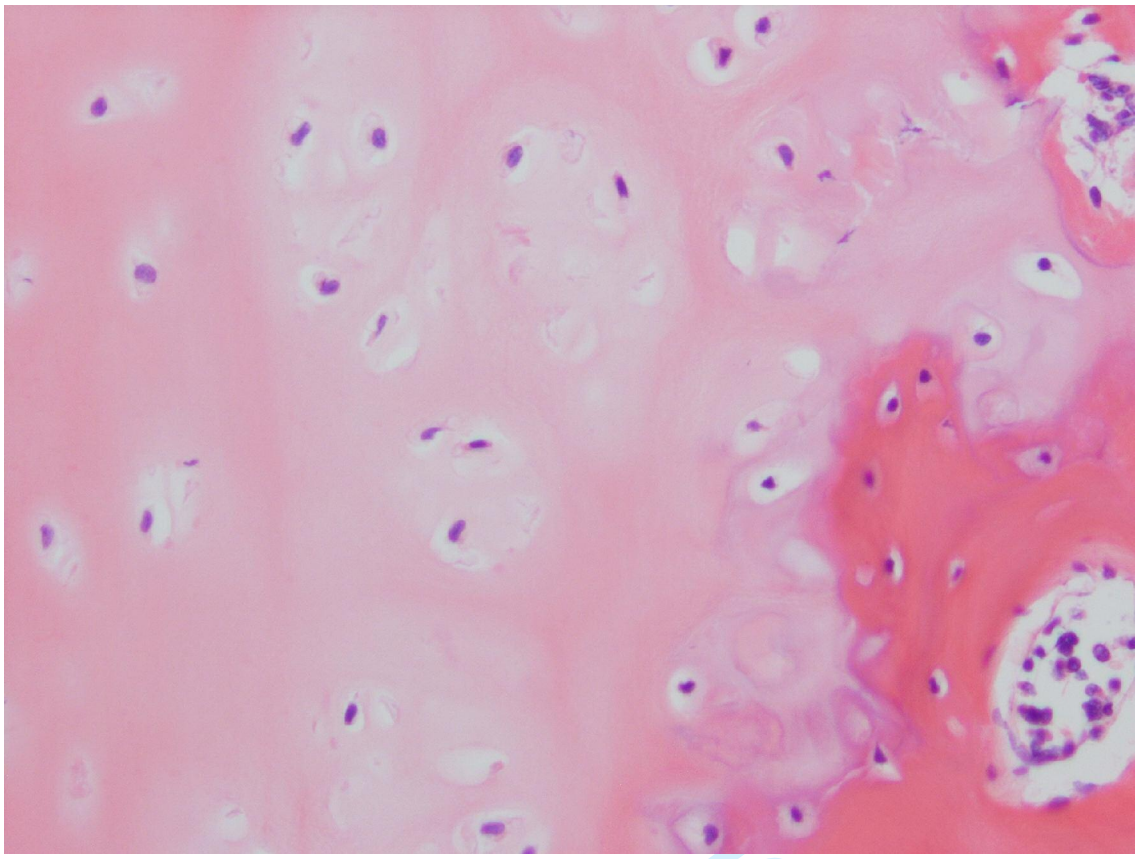

Figure 4. Masson Trichrome Stain x400 from Concave Side of Vertebral Body Growth Plate in Idiopathic Scoliosis Patient # 3.

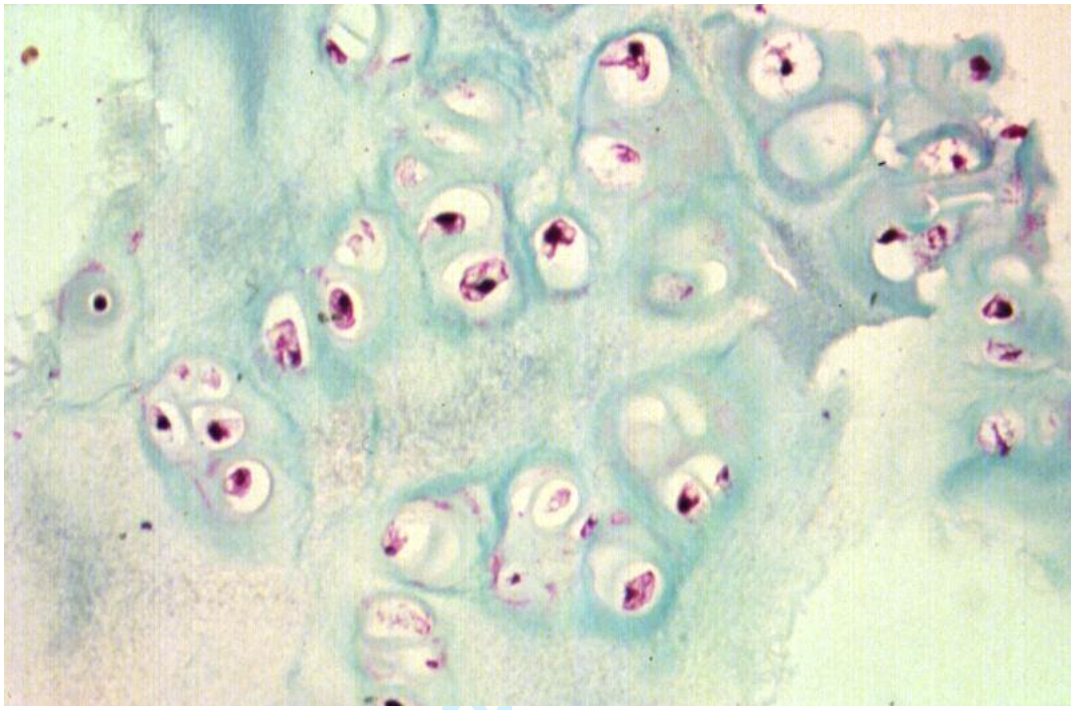

Table 2 Statistical Analysis (Congenital versus Idiopathic Samples) Summary

Levene's Statistic	p-value	T-Statistic	p-value	Mean Difference	SE difference
3.59	0.131	3.43	0.027	3.53	1.03

Table 3 Total RNA Yield & Integrity Summary

Sample Type	Mean [RNA]	Mean 260:280
Idiopathic	87.62ng/uL	1.80-1.90AU
Congenital	72.67ng/uL	1.80-2.00AU

Figure 5. Melt Analysis Demonstrating Successful SHOX Amplification

A = No Template Control, B = 18S and C = SHOX.

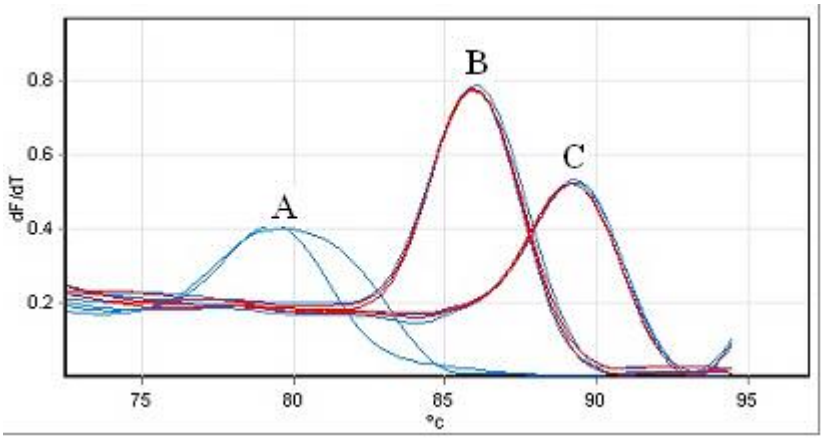

Figure 6 Agarose Gel Electrophoresis of SHOX PCR Products - Muscle.

Lanes 1 – 6 = 18S

Lanes 7 – 12 = SHOX Amplicon

Lanes 13 – 14 = No Template Control

1 2 3 4 5 6 7 8 9 10 11 12 13 14

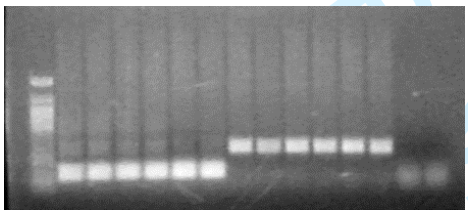

Figure 7 Real-Time Amplification of SHOX

A = 18S, B = SHOX, C=No Template Control

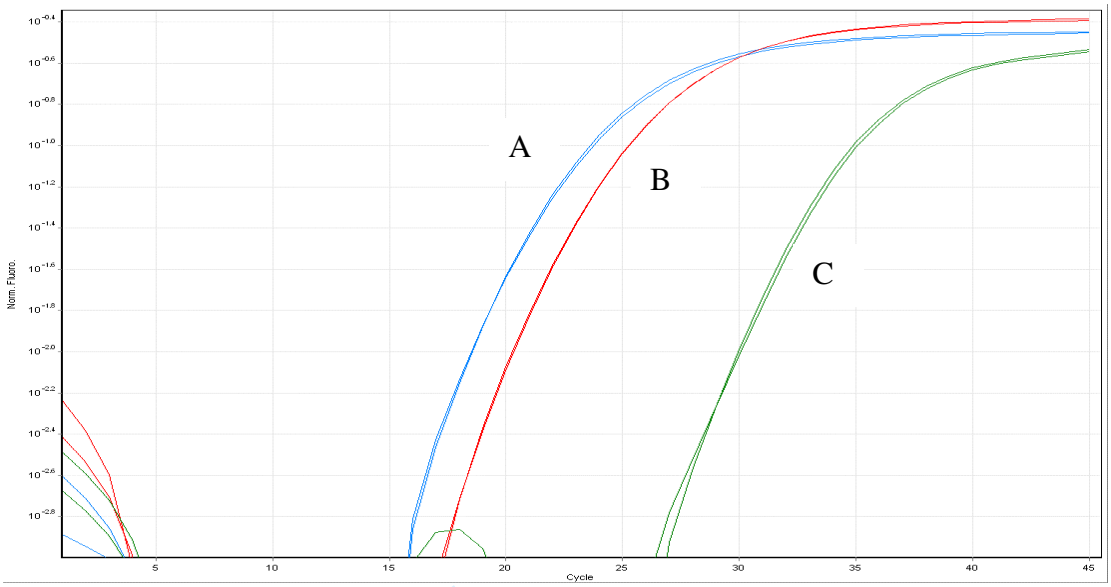

Figure 8 Melt Curve Showing Distinct SHOX Product in Idiopathic Samples

A = No Template Control, B = 18S, C = SHOX.

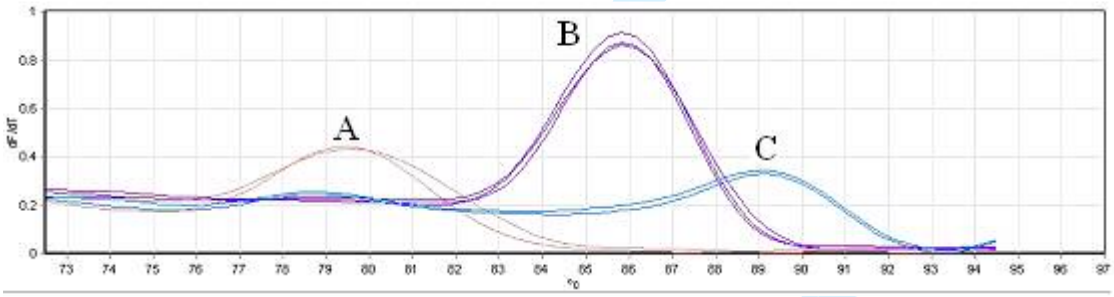

Figure 9. Agarose Gel Electrophoretic Patterns of SHOX Amplicons in Congenital and Idiopathic Scoliosis Vertebral Growth Plates.

Lanes 1 – 6 = 18S

Lanes 7 – 9 = SHOX in Congenital Scoliosis Vertebral Growth Plates

Lanes 10 – 12 = SHOX in Idiopathic Scoliosis Vertebral Growth Plates

Lanes 13 – 14 = No Template Control

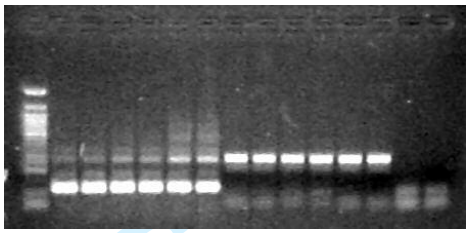

1 2 3 4 5 6 7 8 9 10 11 12 13 14

Table 4. Statistical Analysis of SHOX Expression in Idiopathic vs Congenital Scoliosis.

Vertebral body growth plates	Average Ct	SD	CV
Congenital scoliosis	19.86	1.72	0.09
Idiopathic scoliosis	16.33	0.45	0.03

$2^{-\text{mean}(\Delta\Delta CT)}$ Ratio of Idiopathic to Congenital Scoliosis Expression ↑ 11.52-Fold.

SD = Standard Deviation
CV = Coefficient of Variation